JOURNAL OF OPTIMIZATION THEORY AND APPLICATIONS: Vol. 67, No. 3, DECEMBER 1990

New General Guidance Method in Constrained Optimal Control, Part 2: Application to Space Shuttle Guidance[1,2]

B. KUGELMANN[3] AND H. J. PESCH[4]

Communicated by D. G. Hull

Abstract. The application and the performance of the neighboring optimal feedback scheme presented in Part 1 of this paper is demonstrated for the heating-constrained cross-range maximization problem of a space-shuttle-orbiter-type vehicle. This problem contains five state variables, two control variables, and a state variable inequality constraint of order zero.

Key Words. Neighboring extremals, accessory minimum problem, feedback controls, neighboring optimum guidance, multiple shooting, guidance of space vehicles, space shuttle.

1. Introduction

In Part 1 of this paper, a numerical method for the real-time computation of neighboring optimum feedback controls is developed. In order to demonstrate the practical applicability and efficiency of this feedback scheme, we apply our method to a space flight optimization problem which describes the cross-range maximal reentry of a space-shuttle-type vehicle under a reradiative heating constraint. We have chosen this problem, since it served for many years as one of the most demanding real-life applications

[1] This research was supported in part by the Deutsche Forschungsgemeinschaft under the Schwerpunktprogramm "Anwendungsbezogene Optimierung und Steuerung."

[2] The authors wish to express their sincere and grateful appreciation to Professor Roland Bulirsch who encouraged this work.

[3] Akademischer Rat, Department of Mathematics, University of Technology, Munich, Germany.

[4] Akademischer Rat, Department of Mathematics, University of Technology, Munich, Germany; and Professor of Mathematics, Faculty of Computer Science, University of the Armed Forces, Munich, Germany.

0022-3239/90/1200-0437$06.00/0

during the development of the multiple shooting code (Refs. 1, 2, 3, and 4). The model itself goes back to a paper of Dickmanns (Ref. 5), who also obtained a rather crude approximation for the solution of the unconstrained problem. The heating-constrained problem was completely solved by means of multiple shooting (see Refs. 6, 7, and 8). The accompanying flight path correction problem was treated in Ref. 9 for the unconstrained case.

2. Mathematical Model

Increased range capacity for a space-shuttle-orbiter-type vehicle allows more frequent returns from the orbit. Therefore, the functional chosen to be maximized is the cross-range angle

$$\min I[u] = \min -\Lambda(t_f), \tag{1}$$

subject to the equations of motion (state variables: $x_1 = V \triangleq$ velocity, $x_2 = \chi \triangleq$ heading angle, $x_3 = \gamma \triangleq$ flight path angle, $x_4 = \Lambda \triangleq$ cross-range angle, $x_5 = h \triangleq$ altitude, the down-range angle Θ is decoupled; control variables: $u_1 = \mu \triangleq$ bank angle, $u_2 = C_L \triangleq$ lift coefficient)[5]

$$\dot{V} = -(C_{D_0} + C_L^n)(F\rho_0/2m)\exp(-\beta h)V^2 - g_0[R/(R+h)]^2 \sin\gamma, \tag{2a}$$

$$\dot{\chi} = C_L(F\rho_0/2m)\exp(-\beta h)V(\sin\mu/\cos\gamma) - [V/(R+h)]\cos\gamma\cos\chi\tan\Lambda, \tag{2b}$$

$$\dot{\gamma} = C_L(F\rho_0/2m)\exp(-\beta h)V\cos\mu - \{(g_0/V)[R/(R+h)]^2 - V/(R+h)\}\cos\gamma, \tag{2c}$$

$$\dot{\Lambda} = [V/(R+h)]\cos\gamma\sin\chi, \tag{2d}$$

$$\dot{h} = V\sin\gamma, \tag{2e}$$

with the constants

$$C_{D_0} = 0.04, \qquad n = 1.86, \qquad R = 6371.2 \text{ km},$$
$$F\rho_0/2m = 3.08 \text{ km}^{-1}, \qquad \beta = 0.145 \text{ km}^{-1},$$
$$g_0 = 9.80665E-03 \text{ km sec}^{-2}.$$

The boundary conditions are

$$V(0) = 7.85 \text{ km sec}^{-1}, \qquad \chi(0) = 0,$$
$$\gamma(0) = -1.25\pi/180, \qquad \Lambda(0) = 0, \qquad h(0) = 95 \text{ km},$$
$$V(t_f) = 1.116 \text{ km sec}^{-1}, \qquad \gamma(t_f) = -2.7\pi/180, \qquad h(t_f) = 30 \text{ km},$$

[5] We hope that the customary notation in flight path engineering, which conflicts with the customary notation in optimal control theory (see Part 1 of this paper), does not lead to any confusion, especially w.r.t. μ, Λ, n, T, and π.

where t_f is unspecified. The somewhat unusual value of n in the induced drag model fits the real drag coefficient of the shuttle model better than a quadratic drag polar (cf. Ref. 5).

Moreover, the following zeroth-order state constraint has to be taken into account, which limits the skin temperature of the vehicle:

$$C_L - C_{LH}(V, h) - \Delta C_{LH} \leq 0, \tag{3}$$

where

$$C_{LH} = \sum_{i=1}^{5} B_i H_i, \qquad B_i = \sum_{j=1}^{4} g_{ij} \bar{h}^{j-1},$$

and

$$H_1 = b^2 h^2 / V^2,$$
$$H_2 = bh/V - H_1,$$
$$H_3 = 1 - bh/V - H_2,$$
$$H_4 = V/(bh) - 2 + bh/V - H_3,$$
$$H_5 = V^2/(bh)^2 - 3V/(bh) + 3 - bh/V - H_4,$$
$$\bar{h} = h/50 - 1,$$
$$b = 0.095,$$

and the coefficient matrix

$$g_{ij} = \begin{bmatrix} 0.110717 & 0.834519 & 1.213679 & -1.060833 \\ -0.672677 & 2.734170 & -0.864369 & -12.100000 \\ 0.812241 & 2.337815 & 10.316280 & 22.974860 \\ -3.151267 & -13.621310 & -40.485500 & -57.833330 \\ 2.368095 & 19.073400 & 69.869050 & 127.777778 \end{bmatrix}.$$

Different levels of limit skin temperature T are indicated by the parameter ΔC_{LH} via

$$T = 1093 + 3704 \Delta C_{LH} (^\circ\text{C}).$$

The parameter ΔC_{LH} plays an important role for the computation of the optimal trajectories. Starting with a value of $\Delta C_{LH} \approx 0.12$, the heating constraint is not active (see Fig. 1). Then, by homotopy (i.e., by decreasing the value of ΔC_{LH} in sufficiently small steps), a family of optimal control problems is constructed. The solution of each problem of this so-called homotopy chain serves as an initial guess for the subsequent problem. Notice that the multiple shooting algorithm is essentially a Newton iteration and requires a good starting trajectory. This procedure enables the computation of the constrained problem when the switching structure depends sensitively upon the tightness of the constraint. Details for speeding up this homotopy procedure can be found in Ref. 8.

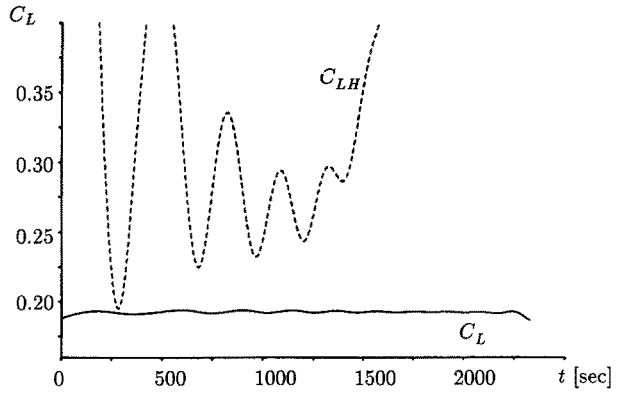

Fig. 1. History of the lift coefficient for $\Delta C_{LH} = 0.12$ (unconstrained case).

To avoid blowing up the paper, the discussion of the necessary conditions of optimal control theory is restricted to the expressions for the optimal control variables in terms of the state and adjoint variables. They are obtained from the first and second variation. The following relations hold:

$$\sin \mu = -\lambda_\chi/(w \cos \gamma), \tag{4a}$$

$$\cos \mu = -\lambda_\gamma/w, \tag{4b}$$

where

$$w = [(\lambda_\chi/\cos \gamma)^2 + \lambda_\gamma^2]^{1/2}$$

and

$$C_L = \begin{cases} C_L^{\text{free}} = [-w/(V\lambda_V nk)]^{1/(n-1)}, & \text{on unconstrained arcs,} \\ C_L^{\text{bound}} = C_{LH}(V, h) + \Delta C_{LH}, & \text{on constrained arcs.} \end{cases} \tag{5}$$

Now, we discuss in brevity the effect of the limitation of the skin temperature. The oscillatory behavior typical for trajectories under entry conditions not corresponding to quasi-steady glide is smoothed with an increasing tightness of the constraint, i.e., a decreasing homotopy parameter ΔC_{LH} (see Fig. 2) as long as the range of ΔC_{LH} is physically significant. The utmost value of $\Delta C_{LH} \approx -0.04566259$ represents the end of the homotopy chain corresponding to a temperature $T \approx 924°C$. Beyond this point, optimal solutions do not exist, since C_L^{free} becomes undefined for nonnegative values of λ_V. Figures 1, 3, and 4 show the time histories of the lift coefficient for different levels of the temperature. Each graph contains two curves—a solid one for the active control, which equals C_L^{free} on unconstrained arcs and C_L^{bound} on constrained arcs, and a dashed one for

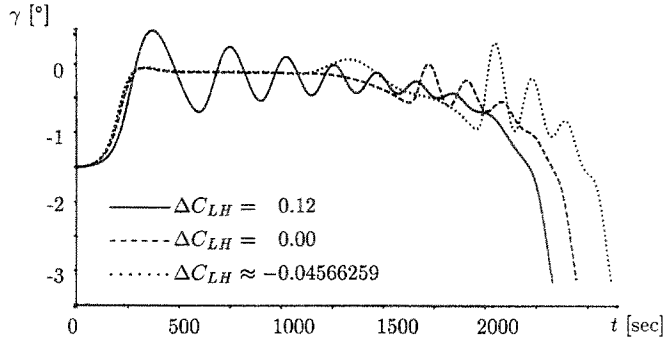

Fig. 2. History of the flight path angle for $\Delta C_{LH} = 0.12, 0.00, -0.04566$.

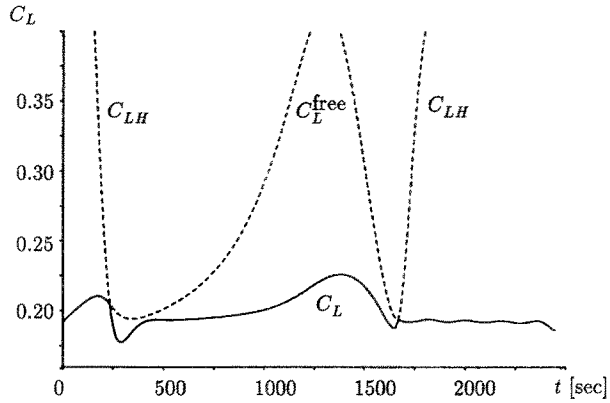

Fig. 3. History of the lift coefficient for $\Delta C_{LH} = 0.00$ (most interesting case).

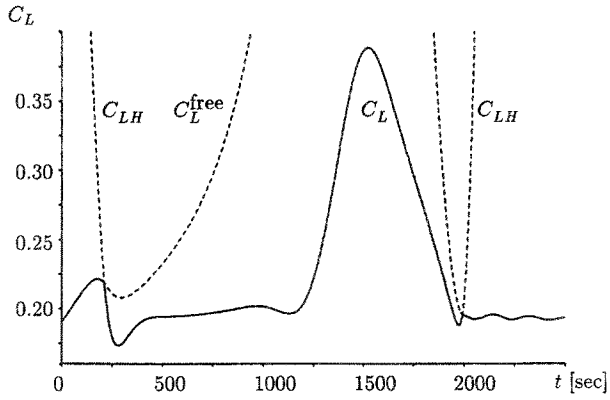

Fig. 4. History of the lift coefficient for $\Delta C_{LH} \approx -0.04566259$ (end of homotopy).

the competitive control which is determined vice versa. Figure 1 shows that a considerably changing switching structure has to be expected when decreasing the parameter ΔC_{LH}. Indeed, the optimal solutions have one to four constrained subarcs. A fifth subarc which might be expected does not occur, since the fifth local minimum is smoothed out during the homotopy. As indicated in Fig. 3, the last two subarcs always merge together (see Ref. 6).

3. Application of the Guidance Method

Now, we give the explicit expressions for the matrices representing the linear multipoint boundary value problem of Section 3 of Part 1 of this paper, in order to establish the feedback scheme.

We find that

$$B = \begin{matrix} {}^{3} \\ {}_{5} \\ {}_{1} \end{matrix} \begin{matrix} \overset{5}{\left[\begin{matrix} \tilde{I} \\ 0 \\ -\dot{\lambda}_0(t_{f_0})^{\mathrm{T}} \end{matrix}\right.} & \overset{5}{\begin{matrix} 0 \\ I \\ \dot{x}_0(t_{f_0})^{\mathrm{T}} \end{matrix}} & \overset{3}{\begin{matrix} 0 \\ -\tilde{I}^{\mathrm{T}} \\ 0 \end{matrix}} & \overset{1}{\left.\begin{matrix} \tilde{I}\dot{x}_0(t_{f_0}) \\ \dot{\lambda}_0(t_{f_0}) \\ 0 \end{matrix}\right]} \end{matrix},$$

where

$$\tilde{I} = \begin{bmatrix} 1 & 0 & 0 & 0 & 0 \\ 0 & 0 & 1 & 0 & 0 \\ 0 & 0 & 0 & 0 & 1 \end{bmatrix},$$

and

$$C_i = {}_{1}\overset{5}{[}W_x, \overset{5}{W_\lambda}, \overset{1}{\dot{W}}]\big|_{t=t_{i_0}},$$

with i denoting the number of the switching point and $\bar{q} = 0$, and

$$D_1 = {}_{10}\overset{10}{[}I, \overset{1}{0}].$$

The switching function W is defined by

$$W = C_L^{\text{free}} - C_L^{\text{bound}}.$$

Furthermore, the rows of B with numbers 4, 6, and 8 can be cancelled, i.e., the parameters $d\nu$ are redundant according to the prescribed terminal conditions.

The performance of the guidance method for this optimal control problem can now be characterized by the size of a multi-dimensional tube

around the optimal trajectory, the so-called controllability tube. Cross sections of this tube are associated with the so-called controllability regions indicating the deviations of a single state variable, either in the positive or in the negative direction which can be successfully compensated for, if all other state variables are assumed to be undisturbed. Of course, this representation by means of controllability regions does not imply that simultaneous disturbances of different state variables cannot be damped out. The boundaries of these regions are obtained by an a posteriori check which accepts the actual trajectory if the final conditions and the heating constraint are not violated beyond a prescribed tolerance. The tolerances are given by the values of the admissible maximum deviations from the prescribed final conditions:

$$\Delta V_f = 0.005 \text{ km sec}^{-1}, \qquad \Delta\gamma_f = 0.03\pi/180, \qquad \Delta h_f = 1 \text{ km}.$$

The heating constraint was considered to be unsatisfied if

$$W(x, \lambda)/(C_{LH} + \Delta C_{LH}) > 0.01.$$

Figures 5 and 6 project the controllability regions w.r.t. velocity and flight path angle due to a slightly constrained subproblem with two switching points and a more severely constrained one with the maximum number of eight switching points. The boundaries have the complicated shape typical for the domain of convergence of iteration methods. All controllability regions first grow and then shrink, which is explained as follows. In the first half of the flight maneuver, the vehicle flies at supersonic speed of more than 5 km/sec, preventing the successful compensation of large deviations. The controllability regions swell when the velocity decreases faster, and then shrink at the end of the flight, because the prescribed final

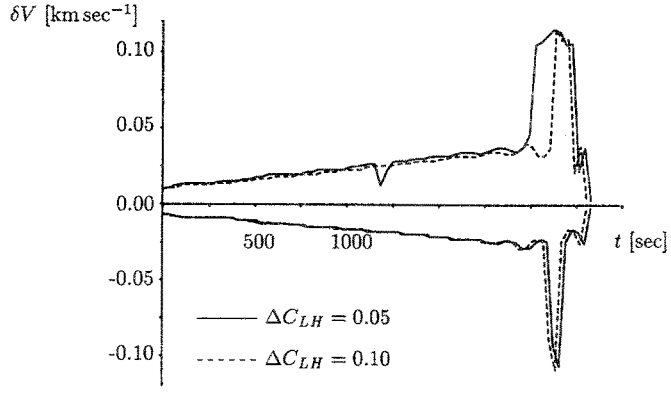

Fig. 5. Controllability regions of velocity for $\Delta C_{LH} = 0.10, 0.05$.

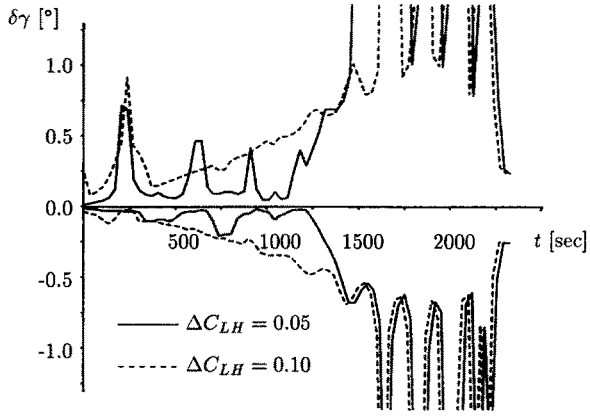

Fig. 6. Controllability regions of flight path angle for $\Delta C_{LH} = 0.10, 0.05$.

conditions force the nonnegative and nonpositive controllability boundaries to merge. The contractions of the controllability tube are related to the location of the constrained subarcs. The sawtoothed behavior of the boundaries beyond the constrained subarcs might be influenced by the oscillations at lower speeds. The same behavior can be found in the numerical results of Refs. 9 and 10. Figures 7 and 8 show comparisons between actual and nominal flight path angle and lift coefficient for a deviation of δh (300 sec) = 4 km.

If perturbed terminal conditions are considered (e.g., for the unconstrained reentry problem), the changes of the end conditions can be compensated successfully for almost all $t_0 < t_{f_0}$ if they stay within the following

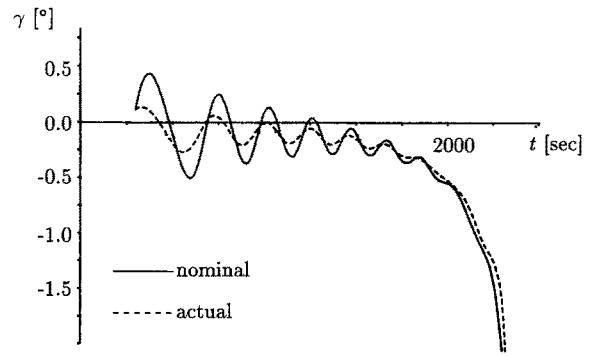

Fig. 7. History of actual and nominal flight path angle for $\Delta C_{LH} = 0.10$ for the deviation δh (300 sec) = 4 km.

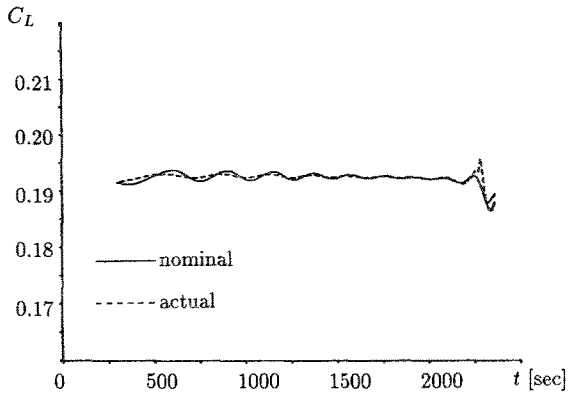

Fig. 8. History of actual and nominal lift coefficient for $\Delta C_{LH} = 0.10$ for the deviation δh (300 sec) = 4 km.

bounds:

$$-25 \text{ m/sec} \leq dV_f \leq 4.5 \text{ m/sec}, \qquad |d\gamma_f| \leq 0.025\pi/180,$$
$$-600 \text{ m} \leq dh_f \leq 100 \text{ m}.$$

Here, dV_f, $d\gamma_f$, and dh_f denote the prescribed changes of the terminal values for the velocity, the flight path angle, and the altitude, respectively.

The region of a good approximation of the optimal control problem by the accessory minimum problem is very limited in this case. This is caused by the high sensitivity of the solution w.r.t. changes of the terminal conditions. Notice that this type of perturbation forces the neighboring extremals to move away from the nominal extremal in the entire time interval. Therefore, this laced controllability tube w.r.t. perturbed terminal conditions may also occur when other guidance schemes are used if these are based on information from a reference trajectory. This also includes all boundary-value-problem solvers using an initial guess for the solution which is then iteratively improved. Even the efficient multiple shooting method has a comparably small domain of convergence if the boundary conditions are perturbed. As a remedy, it is recommended to store several trajectories together with their accompanying feedback schemes.

4. Conclusions

The numerical results for the cross-range maximization problem of a space-shuttle glider under a reradiative heating constraint show that, even for this extremely sensitive problem, the range of controllability is large enough for practical applications.

The range of controllability for terminal perturbations is considerably smaller, since it may be inherent for all feedback schemes that use some information from a reference trajectory.

Together with the more costly repeated correction method, two variants of a multiple shooting based guidance method are available which are numerically stable and nearly optimal. These can be applied either to guidance problems requiring extremely fast corrections—the observance of the constraints can only be guaranteed to the first order in this case—or to problems that allow more expensive computations—in which case all the constraints are checked and even a limited absence of measurement data is not disastrous.

References

1. BULIRSCH, R., *Die Mehrzielmethode zur numerischen Lösung von nichtlinearen Randwertproblemen und Aufgaben der optimalen Steuerung*, DLR, Oberpfaffenhofen, Report of the Carl-Cranz Gesellschaft, 1971.
2. STOER, J., and BULIRSCH, R., *Introduction to Numerical Analysis*, Springer, New York, New York, 1980.
3. DEUFLHARD, P., *A Modified Newton Method for the Solution of Ill-Conditioned Systems of Nonlinear Equations with Applications to Multiple Shooting*, Numerische Mathematik, Vol. 22, pp. 289–315, 1974.
4. DEUFLHARD, P., *A Relaxation Strategy for the Modified Newton Method*, Optimization and Optimal Control, Edited by R. Bulirsch, W. Oettli, and J. Stoer, Springer, Berlin, Germany, 1975.
5. DICKMANNS, E. D., *Maximum Range Three-Dimensional Lifting Planetary Entry*, Marshall Space Flight Center, Technical Report No. RM-199, 1972.
6. PESCH, H. J., *Numerische Berechnung optimaler Steuerungen mit Hilfe der Mehrzielmethode dokumentiert am Problem der Rückführung eines Raumgleiters unter Berücksichtigung von Aufheizungsbegrenzungen*, University of Cologne, Diploma Thesis, 1973.
7. DICKMANNS, E. D., and PESCH, H. J., *Influence of a Reradiative Heating Constraint on Lifting Entry Trajectories for Maximum Lateral Range*, Proceedings of the 11th International Symposium on Space Technology and Science, Tokyo, Japan, pp. 241–246, 1975.
8. DEUFLHARD, P., PESCH, H. J., and RENTROP, P., *A Modified Continuation Method for the Numerical Solution of Nonlinear Two-Point Boundary-Value Problems by Shooting Techniques*, Numerische Mathematik, Vol. 26, pp. 327–343, 1976.
9. PESCH, H. J., *Neighboring Optimum Guidance of a Space-Shuttle-Orbiter-Type Vehicle*, Journal of Guidance and Control, Vol. 3, pp. 386–391, 1980.
10. KRÄMER-EIS, P., *Ein Mehrzielverfahren zur numerischen Berechnung optimaler Feedback-Steuerungen bei beschränkten nichtlinearen Steuerungsproblemen*, University of Bonn, Doctoral Dissertation, 1985.